J|A|C|S
ARTICLES
Published on Web 05/18/2005

157 nm Pellicles (Thin Films) for Photolithography: Mechanistic Investigation of the VUV and UV-C Photolysis of Fluorocarbons

Kwangjoo Lee,[†] Steffen Jockusch,[†] Nicholas J. Turro,*[,†] Roger H. French,[‡] Robert C. Wheland,[‡] M. F. Lemon,[‡] Andre M. Braun,[§] Tatjana Widerschpan,[§] David A. Dixon,[||] Jun Li,[⊥] Marius Ivan,[⊗] and Paul Zimmerman*[,△]

Contribution from the Department of Chemistry, Columbia University, New York, New York 10027; DuPont Central Research & Department, Experimental Station, Wilmington, Delaware 19880; Lehrstuhl fuer Umweltmesstechnik, Universitaet Karlsruhe, 76128 Karlsruhe, Germany; Department of Chemistry, University of Alabama, Tuscaloosa, Alabama 35487-0336; William R. Wiley Environmental Molecular Sciences Laboratory, Pacific Northwest National Laboratory, Richland, Washington 99352; Department of Chemistry, University of Ottawa, Ottawa, ON, K1N 6N5, Canada; and International SEMATECH, Austin, Texas 78741

Received September 29, 2004; E-mail: njt3@columbia.edu; paul.zimmerman@intel.com

Abstract: The use of 157 nm as the next lower wavelength for photolithography for the production of semiconductors has created a need for transparent and radiation-durable polymers for use in soft pellicles, the polymer films which protect the chip from particle deposition. The most promising materials for pellicles are fluorinated polymers, but currently available fluorinated polymers undergo photodegradation and/or photodarkening upon long term exposure to 157 nm irradiation. To understand the mechanism of the photodegradation and photodarkening of fluorinated polymers, mechanistic studies on the photolysis of liquid model fluorocarbons, including perfluorobutylethyl ether and perfluoro-2*H*-3-oxa-heptane, were performed employing UV, NMR, FTIR, GC, and GC/MS analyses. All hydrogen-containing compounds showed decreased photostability compared to the fully perfluorinated compounds. Irradiation in the presence of atmospheric oxygen showed reduced photostability compared to deoxygenated samples. Photolysis of the samples was performed at 157, 172, 185, and 254 nm and showed only minor wavelength dependence. Mechanisms for photodegradation of the fluorocarbons are proposed, which involve Rydberg excited states. Time-dependent density functional theory has been used to predict the excitation spectra of model compounds.

Introduction

The semiconductor industry has used photolithography as the main tool in its efforts to obtain higher resolution features on silicon semiconductors. The emergence of 157 nm lithography, based on the F_2 laser, is expected to continue the advance to dimensions less than 45 nm.[1,2] The development of 157 nm lithography has offered significant challenges with the materials involved in the technology. Many of the challenges come from the high energy (7.9 eV) of the 157 nm photons. For example, the current polymer films, called pellicles, that are designed to protect the photomask from interfering with particulate materials during the lithographic process degrade rapidly under irradiation at 157 nm. Materials used for 193 nm pellicles such as Teflon AF or Cytop degrade rapidly at 157 nm.[3−5] An important challenge for the 157 nm photolithography enterprise is development of pellicles that are not only transparent at this short wavelength but also satisfy a number of stringent requirements, including photostability. Pellicles must possess a high photostability to remain transparent and maintain mechanical stability after extended 157 nm irradiation.[6,7] A number of new fluoropolymers have been developed as candidate materials for soft pellicles (polymer pellicles), all of which

[†] Columbia University.
[‡] DuPont Central Research & Department.
[§] Universitaet Karlsruhe.
[||] University of Alabama.
[⊥] Pacific Northwest National Laboratory.
[⊗] University of Ottawa.
[△] International SEMATECH.

(1) Crawford, M. K.; Farnham, W. B.; Feiring, A. E.; Feldman, J.; French, R. H.; Leffew, K. W.; Petrov, V. A.; Qiu, W.; Schadt, F. L.; Tran, H. V.; Wheland, R. C.; Zumsteg, F. C. *Proc. SPIE* **2003**, *5039*, 80.
(2) ITRS Road map and ITRS updates are published by the semiconductor Industry Association and are available to the public at http://public.itrs.net.
(3) French, R. H.; Wheland, R. C.; Qiu, W.; Lemon, M. F.; Zhang, E.; Gordon, J.; Petrov, V. A.; Cherstkov, V. F.; Delaygina, N. I. *J. Fluorine Chem.* **2003**, *122*, 63.
(4) Zimmerman, P. A.; Miller, D.; Whittaker, G. F. A.; Hill, D.; Rasoul, F.; Liu, H.; Blakely, I.; George, G.; Turro, N. J.; Lee, K.; Jockusch, S.; Proctor, A.; Garza, C.; French, R. H.; Wheland, R. C. In *Understanding Degradation Mechanisms of Materials during Exposure at 157 nm: The Search for a New Soft Pellicle Solution*, Proceedings of the 4th International Symposium on 157 nm Lithography, Yokohama, Japan, August, 2003, Watanabe, T., Ed.
(5) Tregub, A.; Eschbach, F.; Powers, J.; Lo, F. C.; Shigematsu, S.; Nakagawa, H. In *Development of Fluoropolymer Membranes Transparent and Resistant to 157 nm Exposure*, Proceedings of the 4th International Symposium on 157 nm Lithography, Yokohama, Japan, August, 2003, Watanabe, T., Ed.

10.1021/ja0440654 CCC: $30.25

Chart 1. Structures of the Model Compounds.

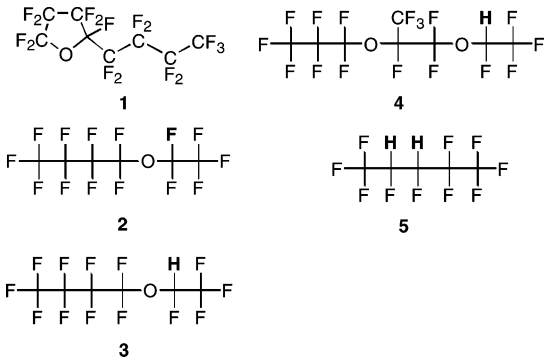

lose transparency due to photodarkening upon irradiation at 157 nm.[3,7,8] Very little information concerning the photochemical mechanisms leading to the photodarkening at 157 nm is currently available.

One of the goals of the research reported here is to publish information that provides insight into the mechanism of the photodegradation processes that leads to the darkening of polymer pellicles during exposure to 157 nm radiation, to enable the design of new soft pellicle systems that possess acceptable characteristics for 157 nm photolithography. A second goal is to invent experimental protocols and strategies for the investigation of photochemistry at 157 nm to set standards for future investigations.

The initial strategy for our investigations was to select a set of model compounds (Chart 1) that are liquids and that possess structures consistent with those of the polymers used in pellicles proposed for use at 157 nm and then to investigate the wavelength dependence of the photolysis of these model compounds as neat liquids. Liquid compounds were studied as a model for initial investigation because they are substantially easier to analyze by techniques, such as gas chromatography, mass spectroscopy, and NMR, due to their relatively low molecular weight in contrast to polymer films. The first part of this paper describes the identification of the products produced by photolysis of the model compounds at various wavelengths of UV radiation (254 nm from a low-pressure Hg lamp, 185 nm from a low-pressure Hg lamp with Suprasil envelope, 172 nm from a noncoherent excimer radiation source, and 157 nm from a F_2 excimer laser). These experiments were designed to determine what photoproducts, if any, are produced by photolysis of small organic model fluorocarbon compounds upon UV irradiation and whether the photolysis at a variety of longer wavelengths produces the same primary products as does photolysis at 157 nm. If the photochemistry of the model compounds is indeed essentially wavelength independent, exploratory studies of the products formed at 157 nm would be greatly facilitated by being able to study reactions at longer wavelengths. The equipment to investigate photolysis at 157 nm irradiation is very specialized and expensive, whereas, for example, photolysis at 185 nm can be achieved with commonly available and much less expensive equipment. Therefore, irradiation at longer wavelength such as 185 nm can be used to prescreen potential candidate materials for pellicles. If no photoproducts were observed after long wavelength irradiation, then tests at 157 nm can be performed.

It should be noted that although the model compounds selected for study in this report are "essentially transparent" at 157 nm, a certain small absorption at longer wavelengths exists for all compounds because of "tailing" of the shorter wavelength absorption spectral feature. The use of liquids and relatively long optical path lengths for photolysis is expected to result in finite absorption which could initiate photochemistry.

Experimental Section

Chemicals. Perfluoro-2-butyltetrahydrofuran (**1**) was purchased from Oakwood Fluorochem USA. Perfluoro butylethyl ether (**2**) and perfluoro-2*H*-3-oxa-heptane (**3**) were synthesized by Exfluor Research Corporation. Freon E2 (**4**) and Vertrel XF (**5**) were obtained from DuPont. All other reagents were obtained from Aldrich and used as received, unless noted otherwise.

Photolysis. Photolysis experiments at 185 and 254 nm were performed in a Rayonet Reactor (Southern New England Ultraviolet), which contains 16 low-pressure Hg lamps using suprasil quartz tubes (3 mm and 10 mm diameter) as sample containers for the VUV photolysis. Deoxygenation of the samples was achieved by five freeze−pump−thaw cycles followed by flame sealing of the samples tube. Photolysis at 157 nm was performed using an Optex excimer laser (Lambda Physik) or a GSI Lumonics excimer laser with F_2 filling. The liquid samples were irradiated in a Harrick demountable liquid IR cell equipped with VUV laser grade CaF_2 windows. Photolysis at 172 nm was performed using a photoreactor equipped with a Xe-excimer lamp as described elsewhere.[9] Deoxygenation of the samples for 157 and 172 nm photolysis was achieved by nitrogen bubbling.

Actinometry. The light intensity of the Rayonet reactor was determined using a calibrated UV power meter (Model: C8026/H8025-185; Hamamadzu). The power at 185 nm at the sample tube position was approximately 0.57 mW/cm^2. Considering the setup geometry of our reactor, the photon exposure of our sample was estimated to be 10 μmol of photons per mL sample in 1 h (6 J/mL hour). Chemical actinometry to determine the irradiance at 172 and 185 nm was performed as described by Braun et al. utilizing the photocleavage of water and scavenging of the generated OH-radicals with methanol.[10] Using this chemical actinometer the light intensity at 185 nm was determined to be 7−9 μmol of photons per mL sample in 1 h (5−6 J/mL h). The energy at 157 nm laser beam was measured using a Molectron JD2000 powermeter ratiometer.

Spectroscopic Characterization. Spectroscopic characterization was performed with the neat samples. UV-vis spectra were recorded using a Shimadzu UV-2401PC UV-vis spectrophotometer. The VUV transmission-based absorbance measurements of the samples were made using a Harrick Scientific Corp. demountable liquid cell (Model DLC-M13). The DLC-M13 was mounted in a VUV-Vase model VU-302 spectroscopic ellipsometer, which is capable of performing transmission measurements (J. A. Woolman Co., Inc., Lincoln, NE). The liquid specimen to be tested was held in a cell formed between parallel CaF_2 windows by insertion of a Teflon ring between the windows. Teflon rings of 6 to 2200 μm thickness were used, providing multiple optical path lengths through aliquots of the sample. The optical absorbance, A (cm^{-1}), per centimeter of specimen thickness is defined for purposes herein as the base 10 logarithm of the ratio of the transmission of the

(6) French, R. H.; Gordon, J. S.; Jones, D. J.; Lemon, M. F.; Wheland, R. C.; Zhang, E.; Zumsteg, F. C., Jr.; Sharp, K. G.; Qiu, W. *Proc. SPIE* **2001**, *4346*, 89.
(7) French, R. H.; Wheland, R. C.; Qiu, W.; Lemon, M. F.; Blackman, G. S.; Zhang, X.; Gordon, J.; Liberman, V.; Grenville, A.; Kunz, R. R.; Rothschild, M. *Proc. SPIE* **2002**, *4691*, 576.
(8) French, R. H.; Wheland, R. C.; Lemon, M. F.; Zhang, E.; Gordon, J. In *Fundamentals of Transparency in Fluoropolymers for use as 157 nm Soft Pellicles*, Proceedings of the 3rd International Symposium on 157 nm Lithography, Antwerp, Belgium, 2002, Van de Hove, L., Ed.
(9) Braun, A. M.; Gassiot Pintori, I.; Popp, H.-P.; Wakahata, Y.; Wörner, M. *Water Sci. Technol.* **2004**, *49*, 235.
(10) Heit, G.; Neuner, A.; Saugy, P.-Y.; Braun, A. M. *J. Phys. Chem. A* **1998**, *102*, 5551.

CaF_2 windows at the test wavelength divided by the transmission at that wavelength of the test sample (windows plus experimental specimen) divided by the thickness of the test specimen. ^1H NMR and ^{19}F NMR measurements were conducted on Bruker NMR spectrometers at 400 and 282.4 MHz, respectively. Sample tubes (containing $CDCl_3$ for locking) with coaxial inserts (containing the sample) were used in both ^1H NMR and ^{19}F NMR measurements. $CFCl_3$ was employed as an internal reference and calibrated as 0 ppm for the ^{19}F NMR experiments. The gas chromatography (GC) analyses were performed on a Varian 3900 gas chromatograph using a Varian Factor FOUR capillary column or a WCOT fused silica column coating with CP-Sil 5 CB LOW BLEED/MS (25 m × 0.25 mm). Gas chromatography/mass spectrometry (GC/MS) was performed on a Varian Saturn 2100 GC/MS instrument using electron ionization. FTIR spectra were recorded on a NEXUS 870 FT-IR (Nicolet) using a Nicolet IR cell with CaF_2 windows.

Calculations. The calculations on CF_3OCF_3, CF_3OCHF_2, $CF_3OCHFCF_3$, and $CF_3CF_2OCHFCF_3$ were done at the density functional theory (DFT) level.[11−14] The geometries were optimized at the local DFT level with Slater exchange[15] and the VWN correlation functional[16] with the DZVP2 basis set.[17] Second derivative calculations showed the predicted structures to be minima. These geometries were used in time-dependent density functional theory (TD-DFT) calculations.[18,19] The TD-DFT calculations were done with the B3LYP functional[20,21] using the new approach to correcting the long-range part of the exchange-correlation function developed by Hirata et al.[22] following the orbital relationships developed by Zhan et al.[23] with the aug-cc-pVDZ basis set[24] augmented by three sets of s, p, d Rydberg functions on the O atom with the exponents 0.005858, 0.003346, and 0.002048 for the s orbitals, 0.009988, 0.005689, and 0.003476 for the p orbitals, and 0.014204, 0.008077, and 0.004927 for the d orbitals. The geometry optimizations were done with the programs Dgauss[25−27] and the TD-DFT calculations with the program NWChem.[28,29] Orbital plots were done with the Ecce extensible computational chemistry environment.[30]

Results and Discussion

After an initial survey of potential candidates for study, the fluorocarbons (**1**−**5**, Chart 1) were selected as model compounds, since they contain important structural units of the most promising polymers such as Cytop and Teflon AF currently proposed for use in soft pellicles[3] and because they could be obtained in high purity. This latter feature is important because we are studying compounds with high transparency in the UV-C and VUV, and impurities could absorb in this region, leading to different chemistry.

The selected fluorocarbons were photolyzed at 254, 185, 172, and 157 nm in the presence and absence of oxygen. The relative photostabilities of the fluorocarbons **1**−**5** were determined by employing several sensitive analytical techniques (UV, NMR, FTIR, GC, and GC/MS). The results are summarized in Table 1 and are mostly based on GC and GC/MS analysis. The plus sign (+) indicates that significant new major signals assigned to photoproducts were observed, the minus sign (−) indicates that no significant major photoproducts were produced under our irradiation condition, and the ± sign means that we are unsure of the result at the given conditions. These results are qualitative and the term "significant" refers to clearly visible GC peaks with reasonable MS fragmentation patterns. From the data in Table 1, an important result is found: the model compounds that contain one or more hydrogen atoms in their structures (e.g., **3**−**5**) more rapidly undergo photodegradation upon UV photolysis as compared to the fully perfluorinated model compounds (e.g., **1** and **2**).

The experimental results using UV, NMR, FTIR, GC, and GC/MS techniques are presented in this paper in detail for **2** and **3** as representative examples. These compounds (perfluorinated ether, **2** and its analogue **3**, which contains hydrogen instead of fluorine at the 2-position) were specifically designed in order to test the influence of hydrogen on the photostability of fluorocarbons in VUV exposure. The photolysis of **2** and **3** were performed both in the presence and in the absence of molecular oxygen in order to investigate whether molecular oxygen is involved in the degradation pathway of perfluorinated or partially fluorinated organic molecules.

In representative experiments, the neat liquid samples of **2** and **3** were placed into suprasil quartz tubes and irradiated at 185 nm for 90 h in the absence (deoxygenated) and in the presence of oxygen (air). After photolysis, a volume decrease was observed for the air saturated samples (**2**: <2%, **3**: 15%) and quartz tubes containing **3** were etched upon photolysis, suggestive of the formation of HF. No measurable volume decrease was observed for the deoxygenated samples, but a color change of samples from clear to light yellow after photolysis at 185 nm of **3**. However, quartz tubes from the photolysis of deoxygenated samples of **2** and **3** showed no sign of etching. Similar results were observed for photolysis at 254 nm of compounds **2** and **3**. The long irradiation times are required to simulate industrial conditions with our model compounds to investigate how the polymers used in the pellicles will break down after many laser pulses.

(11) Hohenberg, P.; Kohn, W. *Phys. Rev. B* **1964**, 864.
(12) Kohn, W.; Sham, L. *J. Phys. Rev. A* **1965**, 140.
(13) Parr, R. G.; Yang, W. *Density-Functional Theory of Atoms and Molecules*; University Press: Oxford, 1989.
(14) Chong, D. P. *Recent Advances in Density Functional Methods*; World Scientific: Singapore, 1995.
(15) Slater, J. C. *Phys. Rev.* **1951**, *81*, 385.
(16) Vosko, S. H.; Wilk, L.; Nusair, M. *Can. J. Phys.* **1980**, *58*, 1200.
(17) Godbout, N.; Salahub, D. R.; Andzelm, J.; Wimmer, E. *Can. J. Chem.* **1992**, *70*, 560.
(18) Bauernschmitt, R.; Ahlrichs, R. *Chem. Phys. Lett.* **1996**, *256*, 454.
(19) Casida, M. E.; Jamorski, C.; Casida, K. C.; Salahub, D. R. *J. Chem. Phys.* **1998**, *108*, 4439.
(20) Becke, A. D. *J. Chem. Phys.* **1993**, *98*, 5648.
(21) Lee, C.; Yang, W.; Parr, R. G. *Phys. Rev. B* **1988**, *37*, 785.
(22) Hirata, S.; Zhan, C.-G.; Apra, E.; Windus, T. L.; Dixon, D. A. *J. Phys. Chem. A* **2003**, *107*, 10154.
(23) Zhan, C.-G.; Nichols, J. A.; Dixon, D. A. *J. Phys. Chem. A* **2003**, *107*, 4184.
(24) Kendall, R. A.; Dunning, T. H.; Harrison, R. J. *J. Chem. Phys.* **1992**, *96*, 6796.
(25) Andzelm, J. W.; Wimmer, E. *J. Chem. Phys.* **1992**, *96*, 1280.
(26) Andzelm, J. W. In *Density Functional Theory in Chemistry*; Labanowski, J. K., Andzelm, J. W., Eds.; Springer-Verlag: New York, 1991; Chapter 11, p 155.
(27) Andzelm, J.; Wimmer, E.; Salahub, D. R. In *The Challenge of d and f Electrons: Theory and Computation*; Salahub, D. R., Zerner, M. C., Eds.; ACS Symposium Series, No. 394, American Chemical Society: Washington D. C., 1989; p 228.
(28) Straatsma, T. P.; Aprà, E.; Windus, T. L.; Bylaska, E. J.; de Jong, W. d.; Hirata, S.; Valiev, M.; Hackler, M.; Pollack, L.; Harrison, R.; Dupuis, M.; Smith, D. M. A.; Nieplocha, J.; Tipparaju, V.; Krishnan, M.; Auer, A. A.; Brown, E.; Cisneros, G.; Fann, G.; Früchtl, H.; Garza, J.; Hirao, K.; Kendall, R.; Nichols, J.; Tsemekhman, K.; Wolinski, K.; Anchell, J.; Bernholdt, D.; Borowski, P.; Clark, T.; Clerc, D.; Dachsel, H.; Deegan, M.; Dyall, K.; Elwood, D.; Glendening, E.; Gutowski, M.; Hess, A.; Jaffe, J.; Johnson, B.; Ju, J.; Kobayashi, R.; Kutteh, R.; Lin, Z.; Littlefield, R.; Long, X.; Meng, B.; Nakajima, T.; Niu, S.; Rosing, M.; Sandrone, G.; Stave, M.; Taylor, H.; Thomas, G.; van Lenthe, J.; Wong, A.; Zhang, Z. *NWChem, A Computational Chemistry Package for Parallel Computers*, 4.6; Pacific Northwest National Laboratory: Richland, WA 99352, 2004.
(29) Kendall, R. A.; Aprà, E.; Bernholdt, D. E.; Bylaska, E. J.; Dupuis, M.; Fann, G. I.; Harrison, R. J.; Ju, J.; Nichols, J. A.; Nieplocha, J.; Straatsma, T. P.; Windus, T. L.; Wong, A. T. *Comput. Phys. Commun.* **2000**, *128*, 260.
(30) Ecce software package from the MSCF, EMSL, PNNL.

Table 1. Summary of Relative Photostabilities Based on GC and GC/MS Analysis of the Selected Model Compounds under Various Irradiation Wavelengths under Air-Saturated or Deoxygenated Conditions

Model compounds		254 nm ~12 000 J	185 nm ~540 J	172 nm ~2 000 J	157 nm ~48 J
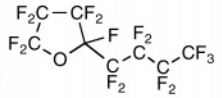 1	air	—	—/+	—	—
	deoxygenated	—	—	—	—/+
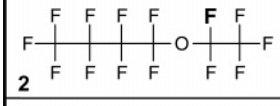 2	air	—	—	—	—
	deoxygenated	—	—	—	—
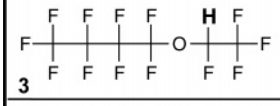 3	air	+	+	+	+
	deoxygenated	+	+	+	+
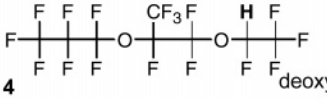 4	air	+	+	+	+
	deoxygenated	+	+	+	+
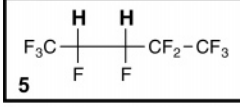 5	air	+	+	+	+
	deoxygenated	+	+	+	+

\+ photoproducts — no photoproducts —/+ not sure

The UV absorption spectra of **2** and **3** upon irradiation at 185 nm are shown in Figure 1. Before irradiation (a, d) the model compounds are nearly transparent in the observed wavelength range. No change in absorbance was observed for **2** after irradiation at 185 nm for 90 h (b) under air-saturated conditions. Conversely, under deoxygenated condition the fully perfluorinated compound **2** showed a significant absorption increase (photodarkening) upon 185 nm photolysis (c). An even stronger absorption increase was observed for **3**, the compound with one hydrogen atom, after irradiation under deoxygenated conditions (f). The absorption extended into the visible spectral region and the yellow color was visible to the eye. Also under air saturated conditions, **3** showed some photodarkening (e). From the UV analysis it can be concluded that the presence of atmospheric oxygen reduces photodarkening. Furthermore, the fully fluorinated compound **2** shows less photodarkening than **3**. No photoproducts could be detected by GC analysis for compound **2** under deoxygenated condition (Table 1). However, the UV spectra (Figure 1, c) showed an increased absorption after irradiation. This indicates that a very small amount of photoproduct was generated, which was not detectable by GC and NMR spectroscopy, but possesses a high molar absorptivity. The air-saturated samples, (b) and (e), tend to give a lower absorbance than the deoxygenated samples, (c) and (f), in Figure 1. We postulate that reaction intermediates, such as radicals, are scavenged in the presence of oxygen, which leads to more transparent photoproducts than in the absence of oxygen.

Compound **2** showed no evidence for significant product formation from FTIR (Figure 2), NMR (Figure 3), and GC (Figure 4) analysis of the samples photolyzed at the irradiation wavelength (254, 185, 172, and 157 nm) that were investigated. Peaks which were initially assigned to impurities in the samples disappeared as the result of photolysis.

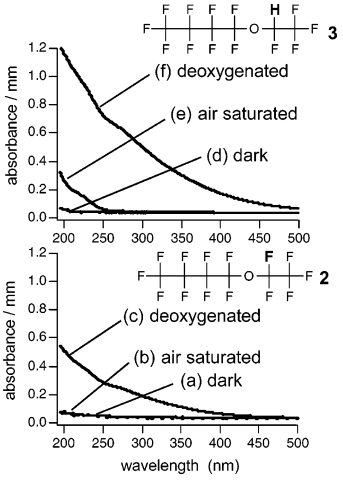

Figure 1. UV-vis spectra of perfluoro butylethyl ether (**2**) (spectra a−c) and perfluoro-2*H*-3-oxa-heptane (**3**) (spectra d−f) upon 185 nm irradiation for 90 h under air-saturated (b, e) and deoxygenated (c, f) conditions.

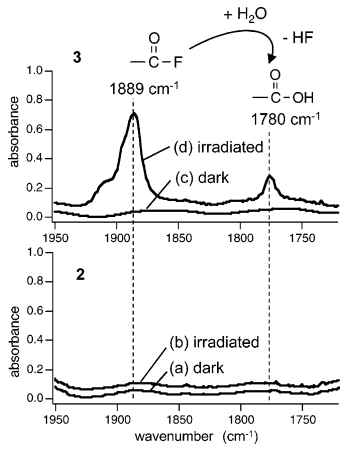

Figure 2. FTIR spectra of **2** (a, b) and **3** (c, d) before (a, c) and after 254 nm irradiation (b, d) under air-saturated conditions in the region of the C=O stretch.

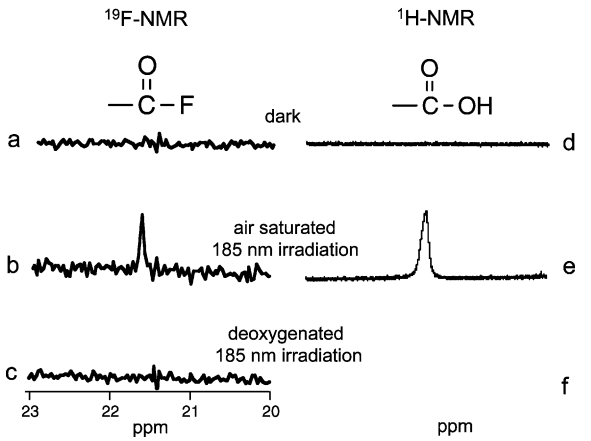

Figure 3. ^{19}F NMR (a−c) and ^{1}H NMR (d−f) **3** before (a, d) and after 185 nm irradiation under air-saturated (b, e) and deoxygenated (c, f) conditions.

A search for photoproducts of perfluoro-2*H*-3-oxa-heptane (**3**) produced upon UV irradiation was made using FTIR, ^{1}H NMR, ^{19}F NMR, GC, and GC/MS techniques. Two characteristic bands were observed from FTIR analysis of the photoproducts of **3** upon irradiation at both 254 and 185 nm under air-saturated conditions, as shown in spectrum (d), Figure 2. These results provide evidence for the occurrence of a carboxylic acid and acid fluoride which have characteristic carbonyl stretching frequencies in the regions of ca. 1780 and 1890 cm^{-1}. The assignments are consistent with results previously reported in the literature.[31] A tentative mechanistic interpretation of the formation of these products is given in Figure 2, where the generated acid fluoride is hydrolyzed by water impurities present in the sample to form carboxylic acids. In addition, NMR analysis showed direct evidence for acyl fluoride and carboxylic acid formation after photolysis of **3** under air saturated conditions. In ^{1}H NMR spectra, a new broad peak at 10 ppm assigned to carboxylic acid (Figure 3e) and, in ^{19}F NMR analysis, a peak at +21.5 ppm assigned to acyl fluoride[32,33] were observed (Figure 3b).

GC/MS analysis of the photolyzed samples of **3** showed significant new peaks (Figure 4). Although MS analysis of the components and structure assignment is nontrivial because of the similar fragmentation patterns of fluorocarbons, two of the components could be assigned with high confidence. On the basis of the mass fragmentation pattern and similarity with published spectra, the carboxylic acids, perfluorobutanoic acid and perfluoropropionic acid, were identified as photoproducts after irradiation of air saturated samples of **3**.

Table 2. TD-DFT Calculations on the Lowest Energy Transitions CF_3OCF_3, CF_3OCHF_2, $CF_3OCHFCF_3$, and $CF_3CF_2OCHFCF_3$

transition energy (eV)	oscillator strength	transition (dominant)
	F_3OCF_3	
10.73	0.008	HOMO → LUMO
11.64	0.001	HOMO → LUMO+1
11.67	0.016	HOMO-1 → LUMO
11.87	0.001	HOMO → LUMO+2
11.88	0.013	HOMO-2 → LUMO
	CF_3OCHF_2	
10.08	0.010	HOMO → LUMO
10.51	0.033	HOMO-1 → LUMO
10.80	0.013	HOMO → LUMO+1
11.01	0.014	HOMO → LUMO+2
	$CF_3OCHFCF_3$	
9.68	0.017	HOMO → LUMO
10.12	0.012	HOMO → LUMO + 1[a]
10.15	0.019	HOMO-1 → LUMO[a]
10.24	0.000	heavily mixed
10.48	0.009	HOMO → LUMO + 2
	$CF_3CF_2OCHFCF_3$	
9.66	0.015	HOMO + LUMO
10.04	0.022	HOMO-1 → LUMO
10.15	0.008	HOMO → LUMO + 1
10.25	0.029	HOMO-2 → LUMO

To get more insight into the photochemistry of the fluorinated compounds during VUV irradiation, the photoabsorption of CF_3OCF_3, CF_3OCHF_2, $CF_3OCHFCF_3$, and $CF_3CF_2OCHFCF_3$ were calculated by using TD-DFT. The results from the TD-DFT calculations are given in Table 2. The calculations show that there are a number of high energy transitions for these compounds. The lowest energy transitions involve excitation of an electron from the HOMO and its nearest neighbors to the LUMO and its nearest neighbors. It is important to remember that in DFT, the HOMO−LUMO gap is close to the first

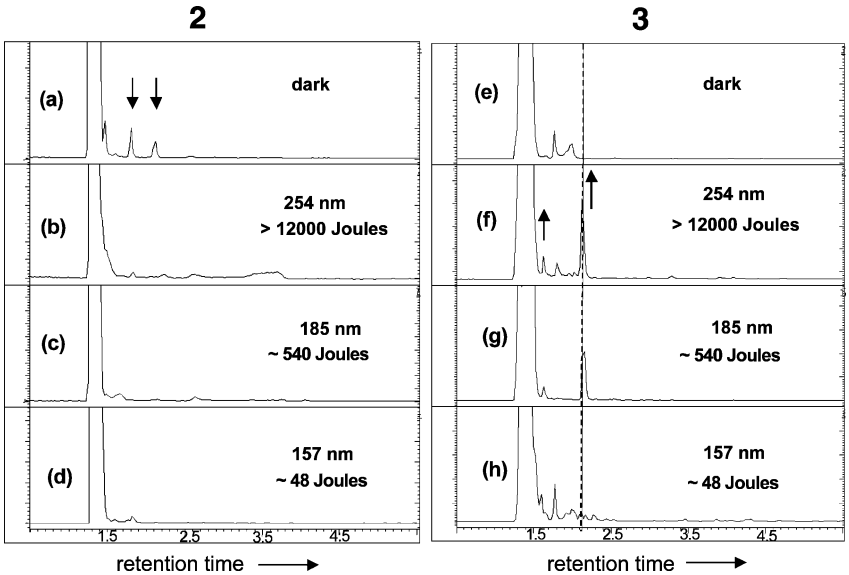

Figure 4. GC analysis of perfluoro butylethyl ether (**2**) and perfluoro-2*H*-3-oxa-heptane (**3**) upon irradiation at various wavelengths. The large peak at 1.2 to 1.6 min corresponds to unreacted **2** and **3**. The small peaks at 1.8 min, 2.2 min (a), and 1.8 min, 2.0 min (e) correspond to impurities.

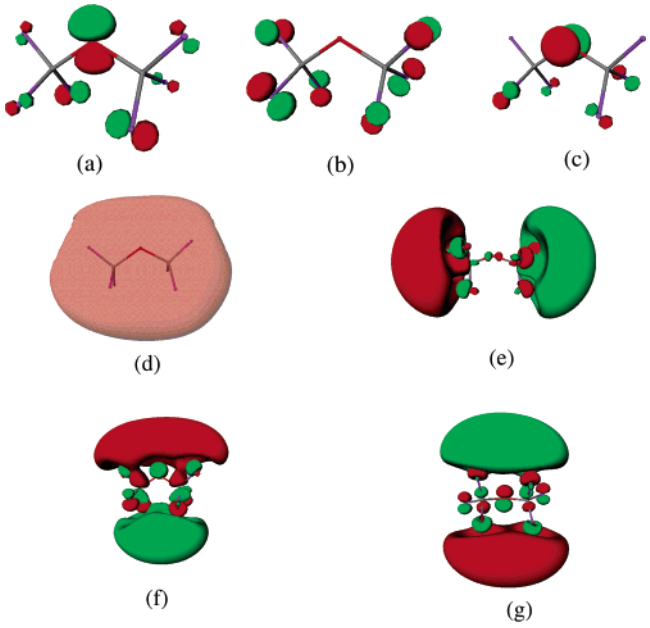

Figure 5. The HOMO, HOMO-1, HOMO-2, and LUMOs of CF_3OCF_3: (a) HOMO-1, (b) HOMO-2, (c) HOMO, (d) LUMO, and (e−g) px, py, and pz Rydberg orbitals, respectively.

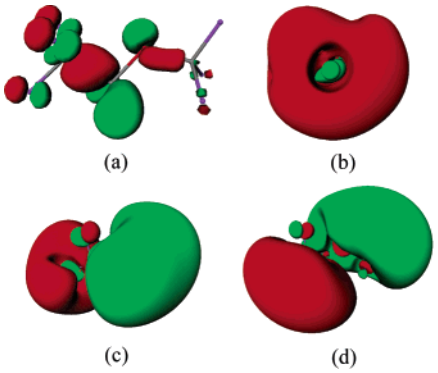

Figure 6. The HOMO and LUMOs of $CF_3OCHFCF_3$: (a) HOMO, (b) LUMO, (c) LUMO+1, (d) LUMO+2 orbital, respectively.

transition energy and that the LUMOs provide information about the excited-state properties. The HOMO, HOMO-1, and HOMO-2 are shown in Figure 5 together with the LUMO and the next 3 lowest lying unoccupied orbitals for CF_3OCF_3. The HOMO and HOMO-2 are predominantly the two lone pair electrons on the O atom, and the HOMO-1 comprises the lone pairs on all of the fluorine atoms. The LUMO is a very diffuse Rydberg s orbital and the next 3 LUMOs are the px, py, and pz Rydberg orbitals. Thus the lowest energy transitions involve promotion of an electron from a lone pair on the oxygen or fluorine atoms to Rydberg orbitals of the molecule. This is consistent with previous calculations of the spectra of these molecules.[22,34] For the molecules with hydrogen, the HOMO is again an oxygen lone pair. The LUMO for CF_3OCHF_2 depends on the conformation of the CHF_2 group and has either distorted s Rydberg character or is a C−H antibonding orbital. The LUMO+1, +2, and +3 are the Rydberg p orbitals. When the CH group is an interior bond, e.g., as in $CF_3OCHFCF_3$ or CF_3-$CF_2OCHFCF_3$, the LUMO is again a Rydberg s orbital and the next orbitals are the Rydberg p orbitals (Figure 6). Thus the best description of the initial excitation process is removal of an electron from a nonbonding orbital to a nearly ionized state leading to an excited state which can be described as a radical cation with a closely affiliated loosely bound electron. If an electron is then transferred from the Rydberg state to a nearby atom, a radical cation would be formed.

The calculated C−O bond energy for CF_3OCF_3 ($CF_3OCF_3 \rightarrow CF_3 + OCF_3$) is 107.1 ± 3 kcal/mol at 298 K based on the heat of formation of CF3OCF3 obtained by the DZP/MP2 level[35−37] from the isodesmic reactions ($CF_3OCF_3 + C_2F_6 \rightarrow CF_3OCF_3 + C_2F_6$) and the heat of formation of CF_3O and CF_3 from the NASA tables.[38] This can be compared to the values of 107.0 kcal/mol at 298K and 106.3 kcal/mol at 0 K obtained at the G3 level (MP2) level,[39,40] showing excellent agreement. The DFT bond energies at 0K at the B3LYP/6-311G* level[41,42] and the BP/DZVP2 level[43−46] are 95.7 and 93.1 kcal/mol, respectively, about 10−12 kcal/mol too low. A typical C−H bond energy is between 100 and 105 kcal/mol, and a C−C bond in a perflurocarbon is about 95 kcal/mol. The C−F bond energies for CF_2 groups are significantly higher near 120 kcal/mol and the C−F bond energy of a CHF group is also expected to be higher, near 110 kcal/mol.[47−50] Thus we predict that in **3**, for example, it is possible to cleave the C−C, C−O, and C−H bonds based on the energy available from photoexcitation and the actual bond energies in the incipient radical cation produced on excitation may well be governing the bond-breaking process.

Scheme 1 shows that the products we observed can be readily rationalized in terms of a model based on an initially generated Rydberg state[51] if we hypothesize that the weakest bond in the excited state of **3** is the O−CHF bond. In the absence of molecular oxygen, the resulting alkoxyl radical (**6**) could undergo cleavage of the C−C bond leading to carbon-centered radicals (**7**) and acid fluorides (**8**). Formation of **9** is unlikely

(31) Forsythe, J. S.; Hill, D. J. T.; Logothetis, A. L.; Whittaker, A. K. *Polym. Degrad. Stab.* **1998**, *63*, 95.
(32) Lappan, U.; Fuchs, B.; Geissler, U.; Scheler, U.; Lunkwitz, K. *Polymer* **2002**, *43*, 4325.
(33) Gerhardt, G. E.; Lagow, R. J. *J. Chem. Soc., Perkin Trans. 1* **1981**, 1321.
(34) Zhan, C.-G.; Dixon, D. A.; Matsuzawa, N. N.; Ishitani, A.; Uda, T. *J. Fluorine Chem.* **2003**, *122*, 27.
(35) Møller, C.; Plesset, M. S. *Phys. Rev.* **1934**, *46*, 618.
(36) Pople, J. A.; Binkley, J. S.; Seeger, R. *Int. J. Quantum Chem. Symp.* **1976**, *10*, 1.
(37) Dunning, T. H., Jr.; Hay, P. J. In *Methods of Electronic Structure Theory*; Schaefer, H. F., III, Ed.; Plenum Press: New York, 1977; Ch. 1.
(38) DeMore, W. B.; Sander, S. P.; Golden, D. M.; Hampson, R. F.; Kurylo, M. J.; Howard, C. J.; Ravishankara, A. R.; Kolb, C. E.; Molina, M. J., *Chemical Kinetics and Photochemical Data for Use in Stratospheric Modeling*; Evaluation Number 12, Jet Propulsion Laboratory (JPL) Publication 97-4, JPL, California Institute of Technology: Pasadena, CA, 1997.
(39) Curtiss, L. A.; Raghavachari, K.; Redfern, P. C.; Pople, J. A. *J. Chem. Phys.* **1997**, *106*, 1063.
(40) Curtiss, L. A.; Raghavachari, K.; Redfern, P. C.; Pople, J. A. *J. Chem. Phys.* **1998**, *109*, 7764.
(41) Becke, A. D. *J. Chem. Phys.* **1993**, *98*, 1372.
(42) Lee, C.; Yang, W.; Parr, R. G. *Phys. Rev. B* **1988**, *37*, 785.
(43) Becke, A. D. *Phys. Rev. A* **1988**, *38*, 3098.
(44) Perdew, J. P. *Phys. Rev. B* **1986**, *33*, 8822.
(45) Godbout, N.; Salahub, D. R.; Andzelm, J.; Wimmer, E. *Can. J. Chem.* **1992**, *70*, 560.
(46) Von Ahsen, S.; Willner, H.; Arguello, G. A. *J. Fluorine Chem.* **2004**, *125*, 1057.
(47) Dixon, D. A.; Smart, B. E.; Krusic, P. J.; Matsuzawa, N. *J. Fluorine Chem.* **1995**, *72*, 209.
(48) Dixon, D. A. Unpublished results based on a revision of the heat of formation of C_3F_8, Krespan, C. G.; Dixon, D. A. *J. Fluorine Chem.* **1996**, *77*, 117, initially based on calculations as described but in agreement with the revised experimental value given in Domalski, E. S.; Hearing, E. D. *J. Phys. Chem. Ref. Data* **1993**, *22*, 805, based on a revised heat of formation of NaF.
(49) Smart, B. E.; Dixon, D. A. *J. Fluorine Chem.* **1992**, *57*, 251.
(50) Smart, B. E. In *Organofluorine Chemistry: Principles and Commercial Applications*; Banks, R. E., Smart, B. E., Tatlow, J. C., Eds.; Topics in Applied Chemistry; Plenum Press: New York, 1994; p 57.
(51) Forsythe, J. S.; Hill, D. J. T.; Logothetis, A. L.; Seguchi, T.; Whittaker, A. K *Radiat. Phys. Chem.* **1998**, *53*, 657.

Scheme 1. Proposed Photodegradation Mechanism and Photoproduct Formation of Perfluoro-2*H*-3-oxa-heptane (**3**)

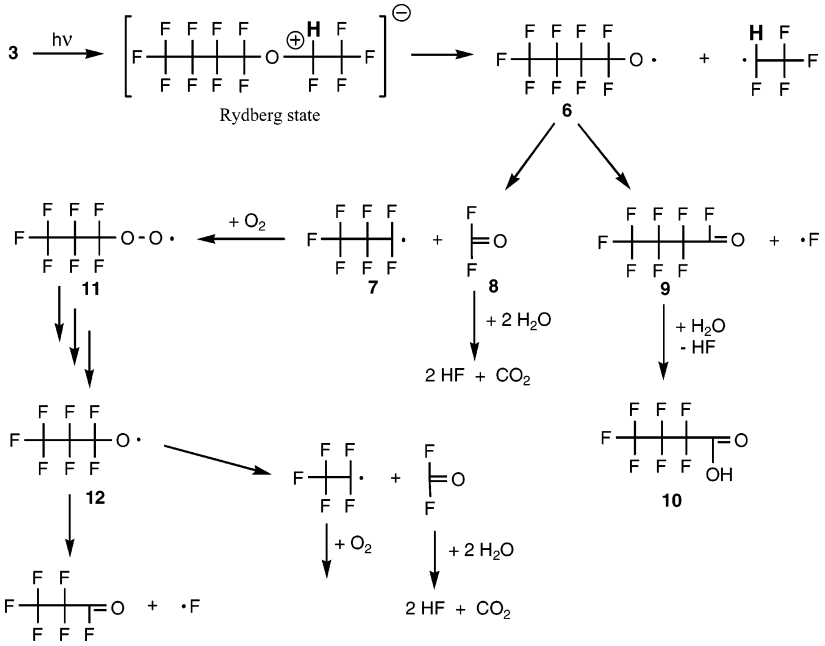

by loss of F path, because the C−F bond-breaking process is endothermic and unlikely in solution, although the path described below when O_2 is present is plausible. A way out of the thermodynamic considerations is for the reaction pathways to be selectively funneled into the C−F bond, i.e., nonrandom vibrational energy transfer. The wavelength independence of product formation does not support this interpretation. Extensive studies of the atmospheric chemistry of hydrofluorocarbons show no evidence for the loss of F radicals from fluorinated alkoxyl radicals because breaking these bonds are quite endothermic processes, whereas cleavage of the C−C bond is near thermoneutral or exothermic with modest barriers.[46,52] C−F bond cleavage could occur if the alkoxyl radical that is produced is vibrationally hot due to its formation but this is unlikely under the current conditions in solution. For example, based on the heat of formation for CF_3CHFO^* generated from the isodesmic reaction $CF_3CHFOH + CH_3O^* \rightarrow CF_3CHFO^* + CH_3OH$ at the MP2/DZP level, the C−F bond dissociation energy in CF_3CHFO^* is 39.2 kcal/mol, the C−H bond dissociation energy is 9.0 kcal/mol, and the C−C bond energy is −6.2 kcal/mol where there is a barrier for the C−C bond dissociation process.[52] More recent calculations place the C−C bond energy to be near 0 ± 2 kcal/mol with a barrier on the order of 10 to 15 kcal/mol.[53,54] Additional bond energy examples include a value of 24.6 kcal/mol for the C−F bond energy in CF_3O and −9.4 kcal/mol for the C−C bond energy in $CF_3CF_2O^*$.[52] Acid fluorides were observed as photolysis products by FTIR and ^{19}F NMR (Figures 2 and 3). The acid fluorides hydrolyze in the presence of water impurities to produce carboxylic acids (**10**), which were directly observed by FTIR (Figure 2), ^1H NMR (Figure 3), and MS. The hydrolysis of the acid fluorides can also generate HF, as evidenced by the etched suprasil quartz tubes. In the presence of atmospheric oxygen, the carbon-centered radicals (**7**) quickly react with the O_2-generating peroxyl radicals (**11**). The peroxyl radicals can then react in a variety of mechanisms leading to the formation of alkoxyl radicals (**12**).[55−57] The resulting alkoxyl radicals (**12**) then undergo subsequent reactions similar to **6**. If O_2 is present in the system, the alkoxyl radicals with C−H bonds can also react with it leading to an overall abstraction of the H atom by the O_2 to form HO_2 and an acid fluoride:

$$CF_3CF_2CHFO^* + O_2 \rightarrow CF_3CF_2CF(O) + HO_2$$

It is also possible to produce HF and an alkene by unimolecular decomposition of an HF species across a C−C bond. Calculated barrier heights at the MP_2/DZP level for HF elimination for the reactions $CHF_2CHF_2 \rightarrow CF_2{=}CHF + HF$, $CF_3CH_2F \rightarrow CF_2{=}CHF + HF$, $CF_3CHF_2 \rightarrow CF_2{=}CF_2 + HF$, and $CF_3CHFCF_3 \rightarrow CF_3FC{=}CF_2 + HF$ are 87.8, 83.6, 93.9, and 82.2 kcal/mol, respectively, less than one-half of the excitation energy at 157 nm.[54]

Conclusion

To understand the mechanism of the photodegradation and photodarkening of polymer pellicles upon exposure to 157 nm irradiation, mechanistic studies on the photolysis of liquid model fluorocarbons **1**−**5** were performed. The hydrogen containing model compounds (**3**−**5**) showed decreased photostability compared to the fully perfluorinated compounds **1** and **2**. There was strong evidence for the formation of HF (etching of the glass tubes) and acid fluorides (IR, GC/MS, NMR) as photoproducts after irradiation of the H-containing compounds **3**−**5** in the presence of atmospheric oxygen. Irradiation of deoxygenated samples **1**−**5** showed increased photodarkening compared to samples irradiated under air-saturated condition.

(52) Dixon, D. A.; Fernandez, R. F. In *Kinetics and Mechanisma for the Reactions of Halogenated Organic Compounds in the Troposphere*; STEP-HALOCSIDE/AFEAS Workshop Proceedings, Sidebottom, H., Ed., University College: Dublin, Ireland, 1993; p 189.
(53) Schneider, W. F.; Wallington, T. J.; Barker, J. R.; Stahlberg, E. A. *Ber. Bunsen-Ges.Phys. Chem.* **1998**, *102*, 1850.
(54) Dixon, D. A. Unpublished results.
(55) Forsythe, J. S.; Hill, D. J. T.; Calos, N.; Logothetis, A. L.; Whittaker, A. K. *J. Appl. Polym. Sci.* **1999**, *73*, 807.
(56) Fisher, W. K.; Corelli, J. C. *J Polym. Sci., Part A: Polym. Chem.* **1981**, *19*, 2465.
(57) Golden, J. H. *J. Polym. Sci. Polym. Chem.* **1960**, *45*, 534.

Consistent with the mechanism of Scheme 1, it can be concluded that the presence of some atmospheric oxygen reduces photodarkening.

A mechanistic interpretation of the photochemical results (Scheme 1) can be made in terms of Rydberg excited states and the known atmospheric degradation chemistry of highly fluorinated alkoxyl radicals. Further calculations on the bond energies of the neutrals, radicals, and radical cations as well as the excitation spectra are needed to validate our mechanistic hypothesis.[34,58]

An important result of our investigation is discovery that the photolysis of a model compound is essentially wavelength independent. This result establishes the possibility that exploratory experiments of the photochemistry of materials which absorb strongly in the VUV may be examined with the much more convenient equipment that is available in the UV-C. The wavelength independence of the condensed phase photochemistry of organic compounds in the visible and UV-A to UV-C regions of the spectrum has been known for many decades (Kasha's Rule).[59] The results reported here indicate that this generalization may tentatively be expanded to the VUV. We note however that the photochemistry could differ from that due to valence band excitation if Rydberg states are involved.

Acknowledgment. The authors thank SEMATECH International for its generous financial support of this work. The authors at Columbia thank the National Science Foundation (Grant NSF-CHE-01-10655) for its financial support. D. A. Dixon thanks the Robert Ramsay Chair Fund for support. A portion of this work was performed in the William R. Wiley Environmental Molecular Sciences Laboratory (EMSL) and part of the work was done using the Molecular Sciences Computing Facility (MSCF) in the EMSL at PNNL. The EMSL including the MSCF is a national user facility funded by the Office of Biological and Environmental Research of the U.S. Department of Energy. The authors would like to thank Prof. J. C. Scaiano for fruitful discussions.

Supporting Information Available: TD-DFT calculations, coordinates, and total energies for the molecules in Table 2. This material is available free of charge at http://www.pubs.asc.org.

JA0440654

(58) Dixon, D. A.; Matsuzawa, N. N.; Ishitani, A.; Uda, T. *Phys. Status Solidi B* **2001**, *226*, 69.

(59) Turro, N. J. *Modern Molecular Photochemistry*; University Science Books: Sausalito, CA, 1976.